

RESEARCH

Open Access



# Chrysoeriol suppresses hyperproliferation of rheumatoid arthritis fibroblast-like synoviocytes and inhibits JAK2/STAT3 signaling

Jia-Ying Wu<sup>1,2,3†</sup>, Ying-Jie Chen<sup>1,2,3†</sup>, Xiu-Qiong Fu<sup>1,2,3</sup>, Jun-Kui Li<sup>1,2,3</sup>, Ji-Yao Chou<sup>1,2,3</sup>, Cheng-Le Yin<sup>1,2,3</sup>, Jing-Xuan Bai<sup>1,2,3</sup>, Ying Wu<sup>1,2,3</sup>, Xiao-Qi Wang<sup>1,2,3</sup>, Amy Sze-man Li<sup>1,2,3</sup>, Lut Yi Wong<sup>1,2,3</sup> and Zhi-Ling Yu<sup>1,2,3,4\*</sup>

## Abstract

**Background:** Fibroblast-like synoviocytes (FLS) have cancer cell-like characteristics, such as abnormal proliferation and resistance to apoptosis, and play a pathogenic role in rheumatoid arthritis (RA). Hyperproliferation of RA-FLS that can be triggered by the activation of interleukin-6/signal transducer and activator of transcription 3 (IL-6/STAT3) signaling destructs cartilage and bone in RA patients. Chrysoeriol is a flavone found in medicinal herbs such as *Chrysanthemum Indici Flos* (the dried capitulum of *Chrysanthemum indicum* L.). These herbs are commonly used in treating RA. Chrysoeriol has been shown to exert anti-inflammatory effects and inhibit STAT3 signaling in our previous studies. This study aimed to determine whether chrysoeriol inhibits hyperproliferation of RA-FLS, and whether inhibiting STAT3 signaling is one of the underlying mechanisms.

**Methods:** IL-6/soluble IL-6 receptor (IL-6/sIL-6R)-stimulated RA-FLS were used to evaluate the effects of chrysoeriol. CCK-8 assay and crystal violet staining were used to examine cell proliferation. Annexin V-FITC/PI double staining was used to detect cell apoptosis. Western blotting was employed to determine protein levels.

**Results:** Chrysoeriol suppressed hyperproliferation of, and evoked apoptosis in, IL-6/sIL-6R-stimulated RA-FLS. The apoptotic effect of chrysoeriol was verified by its ability to cleave caspase-3 and caspase-9. Mechanistic studies revealed that chrysoeriol inhibited activation/phosphorylation of Janus kinase 2 (JAK2, Tyr1007/1008) and STAT3 (Tyr705); decreased STAT3 nuclear level and down-regulated protein levels of Bcl-2 and Mcl-1 that are transcriptionally regulated by STAT3. Over-activation of STAT3 significantly diminished anti-proliferative effects of chrysoeriol in IL-6/sIL-6R-stimulated RA-FLS.

**Conclusions:** We for the first time demonstrated that chrysoeriol suppresses hyperproliferation of RA-FLS, and suppression of JAK2/STAT3 signaling contributes to the underlying mechanisms. This study provides pharmacological and chemical justifications for the traditional use of chrysoeriol-containing herbs in treating RA, and provides a pharmacological basis for developing chrysoeriol into a novel anti-RA agent.

**Keywords:** Apoptosis, Chrysoeriol, JAK2, STAT3 signaling, Proliferation, Rheumatoid arthritis fibroblast-like synoviocytes

## Background

Rheumatoid arthritis (RA) is a chronic inflammatory disease that affects 0.5–1.0% of the global population. RA causes joint damage, disability and other comorbidities, seriously degrading the patients' quality of life

\*Correspondence: zlyu@hkbu.edu.hk

<sup>†</sup>Jia-Ying Wu and Ying-Jie Chen contributed equally to this work.

<sup>2</sup> School of Chinese Medicine, Consun Chinese Medicines Research Centre for Renal Diseases, Hong Kong Baptist University, Hong Kong, China

Full list of author information is available at the end of the article



[1, 2]. Fibroblast-like synoviocytes (FLS) have cancer cell-like characteristics, such as abnormal proliferation and resistance to apoptosis, and play a pathogenic role in RA [3]. Hyperproliferation of RA-FLS leads to the damage of bones and cartilage of RA patients. Activation of signal transducer and activator of transcription 3 (STAT3) promotes proliferation and suppresses apoptosis of RA-FLS [4]. High level of interleukin-6 (IL-6), commonly found in inflamed joints of RA patients, causes abnormal activation/phosphorylation of STAT3 (Tyr705) [5]. Therefore, the IL-6/STAT3 pathway has been regarded as a target for treating RA.

Disease-modifying antirheumatic drugs (DMARDs), including conventional DMARDs (e.g., methotrexate and leflunomide), targeted DMARDs (e.g., Janus kinase inhibitors) and biological DMARDs (e.g., tumor necrosis factor inhibitors, IL-6 inhibitors, IL-1 inhibitors and T-cell immunomodulators), are the mainstay for treating RA [6]. DMARDs can efficiently ameliorate joint swelling and pain of RA patients [7]. However, they have severe adverse effects that have restricted their clinical use. The most severe side effect of DMARDs is infection, a result of their inhibitory effects on the host immune system [8]. Stomach upset, hepatotoxicity, blood dyscrasias and interstitial lung disease are commonly associated with DMARDs as well [9]. Other available anti-RA drugs, including non-steroidal anti-inflammatory drugs (NSAIDs) and glucocorticoids, also have side effects, including cardiovascular, upper gastrointestinal, metabolic and endocrine effects [10, 11]. Developing safe and effective natural products as novel anti-inflammatory agents is a hot research topic in anti-RA drug discovery.

Chrysoeriol (CSR) is a flavonoid compound found in diverse medicinal herbs such as *Cardiospermum halicacabum* Herba (all parts of *Cardiospermum halicacabum* L.) and *Chrysanthemi Indici Flos* (the dried capitulum of *Chrysanthemum indicum* L.) [12, 13]. These herbs are commonly used for treating RA and have been shown to have anti-arthritic effects in animal models [14, 15]. These facts suggest that CSR has anti-arthritic effects. In a previous study, we found that CSR ameliorates 12-O-tetradecanoylphorbol-13-acetate (TPA)-induced acute skin inflammation in mice. Moreover, in the animal model and in RAW264.7 cells, CSR inhibits STAT3 signaling [16]. Whether CSR inhibits proliferation of, and induces apoptosis in RA-FLS is unknown.

In this work, we investigated the effects of CSR on hyperproliferation of IL-6/sIL-6R-stimulated RA-FLS and explored the involvement of the JAK2/STAT3 pathway in the effects.

## Materials and methods

### Reagents

CSR (purity > 99%, determined by HPLC) was purchased from Extrasynthese (Genay Cedex, France). Indomethacin, crystal violet, phosphate-buffered saline (PBS) and dimethylsulfoxide (DMSO) were purchased from Sigma Chemical Co. (St. Louis, MO, USA). CCK-8 (Cell Counting Kit-8) was purchased from TransGen Biotech (Beijing, China). Recombinant human IL-6 and recombinant human soluble IL-6 receptor  $\alpha$  (sIL-6R) were purchased from PeproTech (Rocky Hill, NY, USA). Janus kinase 2 (JAK2, ab39636) and phospho-JAK2 (Tyr1007/1008, ab32101) monoclonal antibodies, HRP-conjugated secondary antibodies (ab7090, ab97040), and Annexin V-FITC Apoptosis Staining / Detection Kit (#ab14085) were purchased from Abcam (Cambridge, CB2 0AX, UK). B-cell lymphoma 2 (Bcl-2, sc-7382) and GAPDH (sc-365062) monoclonal antibodies were obtained from Santa Cruz Biotechnology (Santa Cruz, CA, USA). Myeloid cell leukemia 1 (Mcl-1, #94296), caspase-9 (#9508), caspase-3 (#9662), STAT3 (#12640), phospho-STAT3 (Tyr705, #9131) and lamin B1 (#12586) monoclonal antibodies were obtained from Cell Signaling Technology (Boston, MA, USA). All other chemicals used were purchased from Sigma and were of analytical grade.

### Cell culture

RA-FLS were purchased from Cell Applications (San Diego, CA). L929 and MIHA cells were purchased from American Type Culture Collection (ATCC; Rockville, MD, USA). Fetal bovine serum (FBS) and Dulbecco's Modified Eagle Medium (DMEM) were purchased from HyClone (Logan UT, USA). Cells were maintained in high glucose DMEM containing 10% FBS and 1% penicillin/streptomycin (P/S, GIBCO, USA) at 37 °C in a humidified atmosphere of 5% CO<sub>2</sub>. CSR and indomethacin were dissolved in DMSO at the concentrations of 40 mM and 100 mM, respectively. IL-6 was reconstituted in distilled water to 50  $\mu$ g/ml and sIL-6R was reconstituted in PBS to 50  $\mu$ g/ml (PH 7.2). Solutions for cell assays were filtered with syringe filters (0.22  $\mu$ m) and stored at -20 °C. The stock solutions were diluted with DMEM immediately before experiments. The final concentration of DMSO in cell culture was 0.1%.

### Cell viability assay

CCK-8 assay was performed to determine the cytotoxicity of CSR on RA-FLS, MIHA and L929 cells. Cells ( $3 \times 10^3$ /well) in 200  $\mu$ l DMEM were seeded in 96-well plates, incubated at 37 °C for 24 h and given a fresh medium change. The cells were treated with various concentrations of CSR (0, 5, 10, 20, 40, 80  $\mu$ M) or

indomethacin (100  $\mu$ M) for 1 h and then stimulated with IL-6/sIL-6R (100 ng/ml each) for 24 h or 48 h. Cells in the control group were treated with solvents (DMSO for CSR; PBS for IL-6/sIL-6R). In each well, 20  $\mu$ l of CCK-8 solution was added and then incubated for 4 h. Absorbance of each well was measured at 450 nm with a microplate spectrophotometer (BD Biosciences, USA).

#### Crystal violet staining

The crystal violet staining assay was employed to visualize the effects of CSR on the proliferation of RA-FLS. Cells ( $1 \times 10^6$  cell/dish) seeded in 60 mm dishes were treated with CSR at various concentrations (0, 10, 20  $\mu$ M) for 1 h and stimulated with IL-6/sIL-6R (100 ng/ml each) for 48 h. Afterwards, cells were fixed with 10% formalin for 5 min, followed by staining with 0.05% crystal violet solution in distilled water for 30 min. Cells were then washed and photographed. Crystal violet was solubilized with 1 ml of 33% glacial acetic acid. Absorbance was measured at 570 nm using a microplate spectrophotometer.

#### Apoptosis assay

Apoptotic effects of CSR on RA-FLS were measured by Annexin V-FITC/PI double staining using an Apoptosis Detection Kit following the manufacturer's protocol. Cells ( $1 \times 10^5$  cell/well) were seeded in 6-well plates overnight and then treated as described in the Crystal violet staining section. Both detached and adherent cells were harvested and then incubated in 100  $\mu$ l labeling solution (5  $\mu$ l of Annexin V-FITC, 5  $\mu$ l of PI, 10  $\mu$ l of  $10 \times$  binding buffer and 80  $\mu$ l of  $H_2O$ ) in darkness at room temperature for 15 min. After that, 400  $\mu$ l of  $1 \times$  binding buffer was added to stop the staining reaction. Flow cytometric analysis was then performed with a BD Accuri C6 flow cytometer (BD Biosciences, USA). In the flow cytometric scatter graphs, cells undergoing apoptosis are shown in the upper-right quadrant (late-stage apoptotic cells) and the lower-right quadrant (early-stage apoptotic cells).

#### Immunoblotting

Lysates were prepared from cultured RA-FLS as previously described [17]. Cell nuclear and cytoplasmic extracts were prepared using the Mammalian Nuclear and Cytoplasmic Protein Extraction Kit (TransGen Biotech, Beijing, China) following the manufacturer's protocol. Protein concentrations were measured using a Quick Start<sup>TM</sup> Bradford Protein Assay (Bio-Rad, USA).

Western blot assays were performed as previously described [16]. Immunoreactive bands were visualized using the Enhanced Chemiluminescence Detection Kit (Invitrogen, USA). Image J software was used to measure the intensity of each band. The relative level of each

protein of interest was normalized to the endogenous  $\beta$ -actin, GAPDH or lamin B1 in each experiment.

#### Adenoviral transduction

Adenovirus expressing green fluorescent protein (GFP)-flag-tagged STAT3C (Ad-STAT3C) and control adenovirus expressing GFP (Ad-Empty vector) were purchased from Vigene Biosciences (Shandong, China). STAT3C (A662C, N664C mutant) is a constitutively activated variant of STAT3. RA-FLS ( $6 \times 10^5$  cells/dish) were seeded in 100 mm dishes and transduced with Ad-STAT3C ( $7.8 \times 10^7$  pfu/ml, RA-FLS<sup>STAT3C</sup>) or Ad-Empty vector ( $7.8 \times 10^7$  pfu/ml, RA-FLS<sup>Empty vector</sup>) for 24 h, and then supernatant was discarded and replaced with fresh medium. After 12 h, transduced RA-FLS were used for experiments.

#### Statistical analysis

Data are presented as the means  $\pm$  standard deviation (SD). Comparison of quantitative data in multiple groups was performed using one-way analysis of variance (ANOVA) followed by Tukey's test.  $P < 0.05$  was regarded as statistically significant.

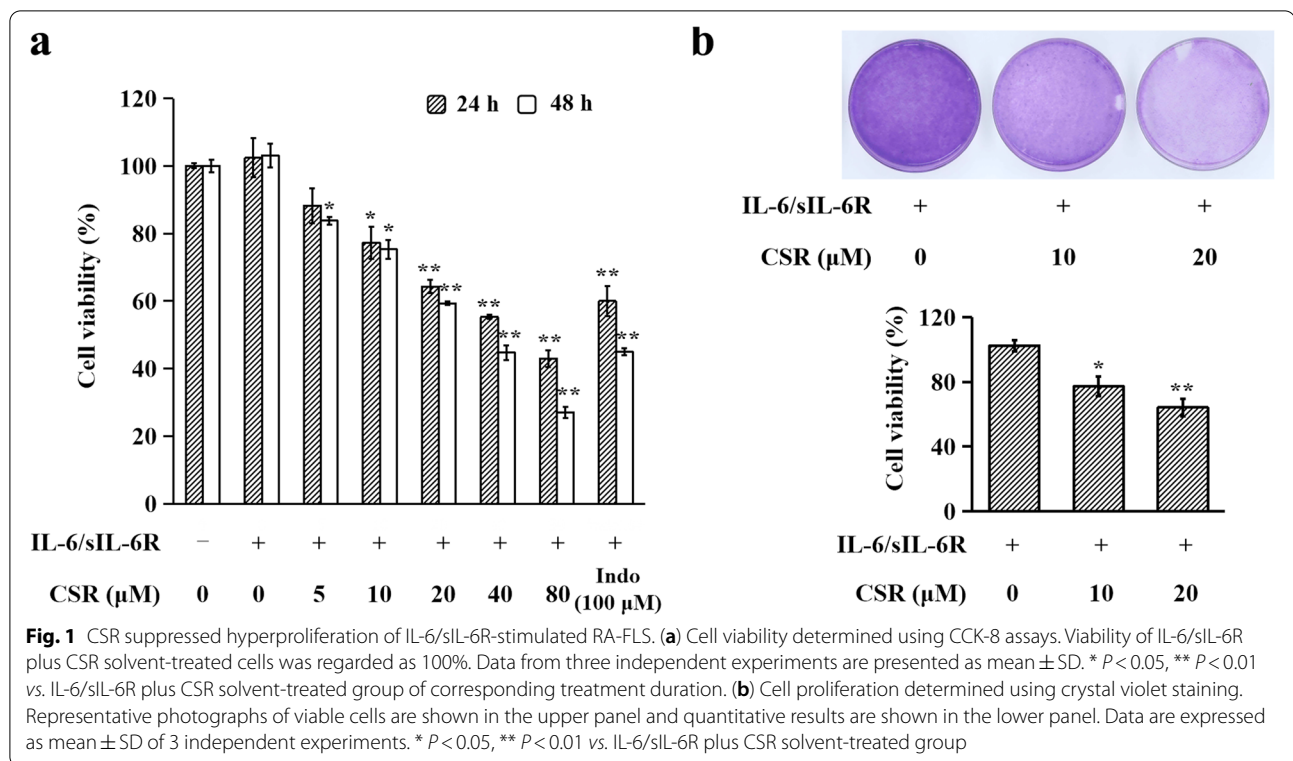
## Results

### CSR suppressed hyperproliferation of IL-6/sIL-6R-stimulated RA-FLS

CCK-8 assay was used to evaluate the effect of CSR on hyperproliferation of IL-6/sIL-6R-stimulated RA-FLS. Results showed that pre-treatments with CSR (5, 10, 20, 40, 80  $\mu$ M; 24 or 48 h) reduced the viability of IL-6/sIL-6R (100 ng/ml each)-stimulated RA-FLS in time- and dose-dependent manners (Fig. 1a). In agreement with previous reports, the positive control drug indomethacin also suppressed the hyperproliferation of IL-6/sIL-6R-stimulated RA-FLS [18]. The anti-proliferative effect of 100  $\mu$ M indomethacin against IL-6/sIL-6R-stimulated RA-FLS was comparable to that of 40  $\mu$ M CSR. Crystal violet staining confirmed that CSR had dose-dependent and significant inhibitory effects on the proliferation of IL-6/sIL-6R-stimulated RA-FLS (Fig. 1b). Anti-proliferative activities of CSR were also evaluated in normal human liver-derived MIHA cells and in mouse fibroblast L929 cells. Viabilities of IL-6/sIL-6R (100 ng/ml each)-stimulated MIHA and L929 cells were not significantly affected by a 24-h incubation with up to 40  $\mu$ M CSR (Additional file 1). These findings indicate that CSR suppresses hyperproliferation of RA-FLS and has no obvious influence on the proliferation of normal cells.

### CSR induced apoptosis in IL-6/sIL-6R-stimulated RA-FLS

Flow cytometry assay was used to determine the pro-apoptotic effects of CSR on IL-6/sIL-6R-stimulated



RA-FLS after Annexin V-FITC/PI double staining. As shown in Fig. 2a, CSR treatments induced cell apoptosis. After a 48-h treatment, apoptosis rates in the control group, low dose CSR group (10  $\mu$ M) and high dose CSR group (20  $\mu$ M) were  $1.4 \pm 0.4\%$ ,  $4.4 \pm 1.5\%$  and  $24.9 \pm 2.9\%$ , respectively. CSR also significantly and dose-dependently elevated protein levels of cleaved caspase-3 and cleaved caspase-9 (Fig. 2b), two apoptotic markers, confirming its apoptotic effects in this cell model.

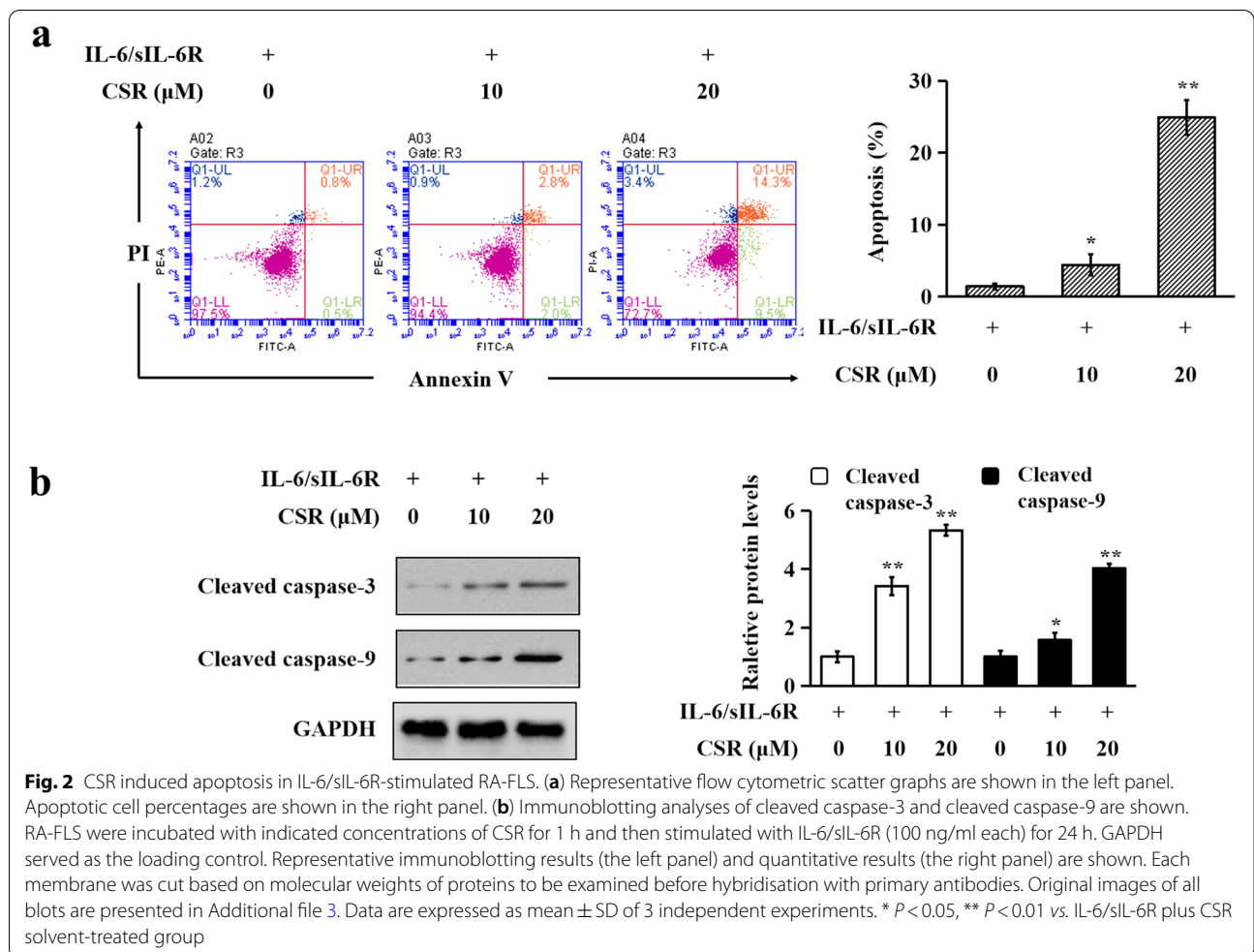
#### CSR inhibited the JAK2/STAT3 pathway in IL-6/sIL-6R-stimulated RA-FLS

As shown in Additional file 2, among 3 tested stimulation durations (20, 40, 80 min) with IL-6/sIL-6R (100 ng/ml each), 40-min stimulation induced the greatest activation/phosphorylation of STAT3 (Tyr705) in RA-FLS. Thus, RA-FLS stimulated with IL-6/sIL-6R (100 ng/ml each) for 40-min were used as the cell model in the subsequent assays. In the present study, we found that pre-treatments of CSR for 1 h dose-dependently inhibited IL-6/sIL-6R-induced phosphorylation of JAK2 (Tyr1007/1008) and STAT3 (Tyr705) without affecting the total JAK2 and STAT3 levels (Fig. 3a). Figure 3b shows that CSR dose-dependently and significantly decreased the nuclear STAT3 level in IL-6/sIL-6R-stimulated RA-FLS. IL-6/sIL-6R alone or in combination with CSR did not affect the protein level of STAT3 in

the cytoplasm. As shown in Fig. 3c, IL-6/sIL-6R upregulated protein levels of Bcl-2 and Mcl-1, which are STAT3 target genes involved in cell survival, while CSR dose-dependently and significantly suppressed the upregulation. These findings indicate that CSR inhibits the JAK2/STAT3 pathway in IL-6/sIL-6R-stimulated RA-FLS.

#### Over-activation of STAT3 attenuated the inhibitory effect of CSR on RA-FLS hyperproliferation

To determine whether STAT3 signaling contributed to the inhibitory effects of CSR on the viability of RA-FLS, we over-activated STAT3 in RA-FLS by transducing STAT3C into the cells. Green fluorescent and bright-field microscopy images of RA-FLS showed that the transduction was successful (Fig. 4a). Immunoblotting showed that transduction with Ad-STAT3C in RA-FLS caused remarkable elevation of phosphorylated STAT3 (Tyr705) level compared to transduction with Ad-Empty vector (Fig. 4a), showing an overactivation of STAT3 in RA-FLS. Upon STAT3 overactivation, the inhibitory effects of 10, 20 and 40  $\mu$ M CSR on the proliferation of IL-6/sIL-6R-stimulated RA-FLS decreased by 9%, 15% and 22%, respectively (Fig. 4b). Viability of CSR-untreated RA-FLS<sup>Empty vector</sup> or CSR-untreated RA-FLS<sup>STAT3C</sup> was regarded as 100%. These findings indicate that inhibition of the STAT3 signaling contributes to the inhibitory effect of CSR on the cell viability of RA-FLS.



## Discussion

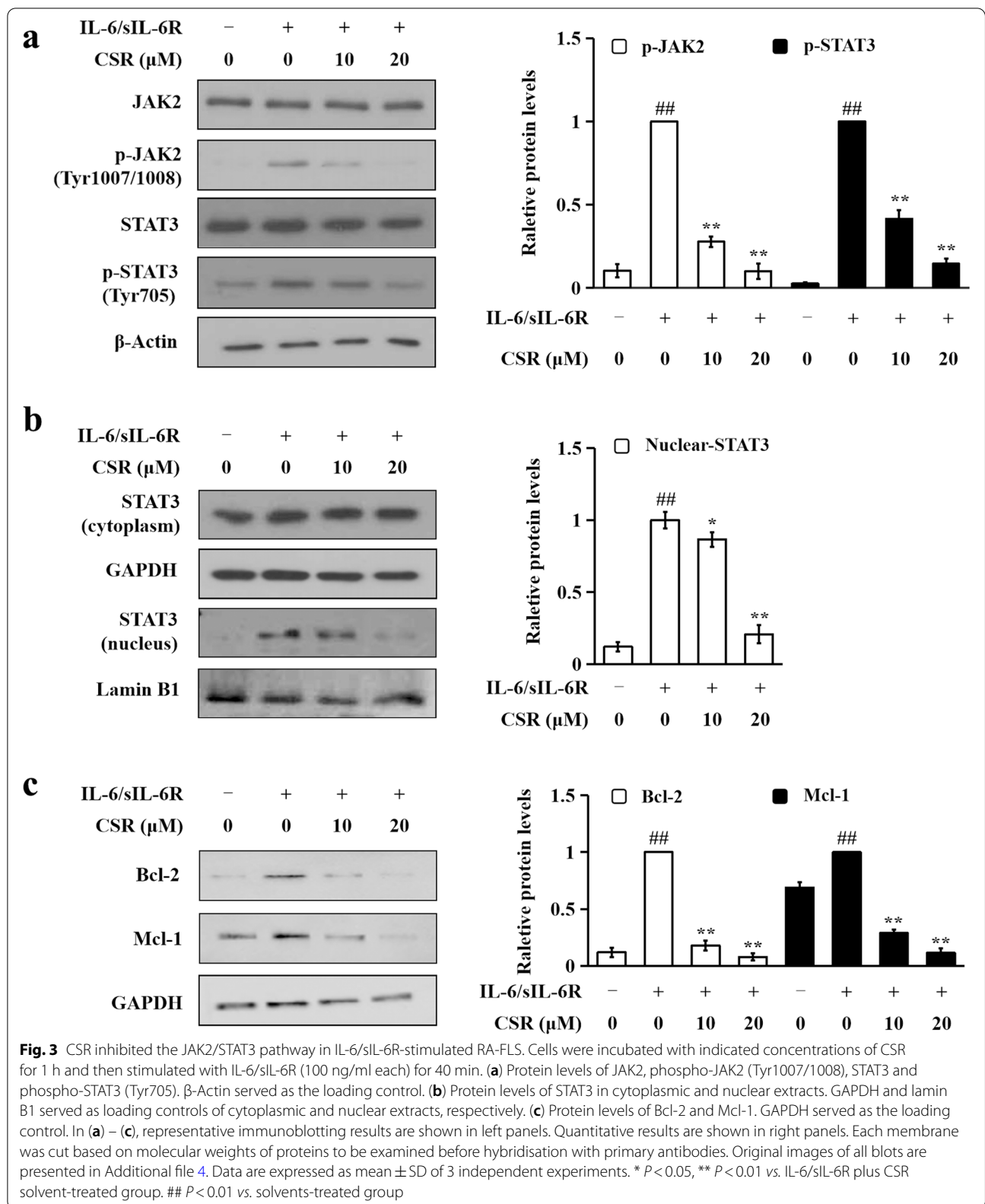
In a previous study, we found that CSR has anti-inflammatory effects in an acute inflammation mouse model [16]. In this study, we demonstrated that CSR inhibits hyperproliferation of RA-FLS. Findings of this and our previous studies suggest that CSR has anti-arthritis potential.

High levels of IL-6 have been observed in joints and blood of RA patients, and serum IL-6 level positively correlates with disease activity [19]. IL-6 exerts its biological activities through IL-6-specific receptor and a signal transducer, gp130 [20]. There are two forms of IL-6-specific receptor: mIL-6R (membrane-bound IL-6R) and sIL-6R. A much higher level of sIL-6R than mIL-6R was detected in synovial fluid and blood of RA patients [21]. Therefore, we used IL-6/sIL-6R-stimulated RA-FLS as the cell model in this study.

When IL-6 binds to sIL-6R in RA-FLS, JAK2, an upstream kinase of STAT3, is activated [22], leading to the activation of STAT3. Activated STAT3 forms

homodimers and then translocates to the nucleus to regulate the transcription of its target genes [23]. By transcriptionally up-regulating survival genes such as Bcl-2 and Mcl-1, STAT3 signaling promotes RA-FLS hyperproliferation [24, 25]. In this study, it was found that CSR lowers protein levels phospho-JAK2 (Tyr1007/1008), phospho-STAT3 (Tyr705), Bcl-2 and Mcl-1 and decreases STAT3 nuclear localization in IL-6/sIL-6R-stimulated RA-FLS, indicating that CSR inhibits the JAK2/STAT3 pathway in the cell model.

Activation of the JAK2/STAT3 pathway promotes FLS activation/proliferation. FLS proliferation and resistance to apoptosis together with recruitment of other fibroblasts result in synovial hyperplasia, a typical feature of RA [26, 27]. During the progression of RA, hyperplastic synovial membrane is of persistent inflammation, leading to cartilage damage and joint destruction [28]. In the present study, CSR was observed to be able to suppress hyperproliferation of, and induce



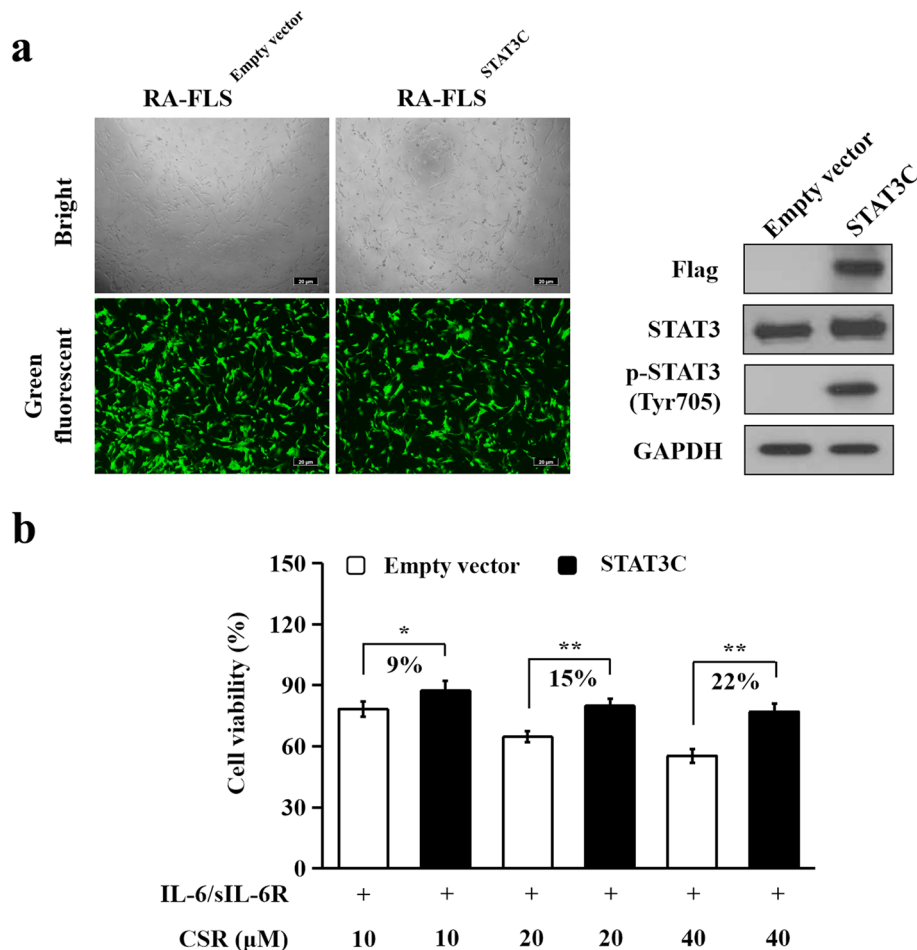


**Fig. 4** Over-activation of STAT3 attenuated the inhibitory effects of CSR on RA-FLS hyperproliferation. RA-FLS were transduced with Ad-STAT3C (RA-FLS<sup>STAT3C</sup>) or Ad-Empty (RA-FLS<sup>Empty vector</sup>) plasmid. **(a)** Green fluorescent protein (GFP) expression and the protein levels of phospho-STAT3 (Tyr 705), STAT3 and Flag in RA-FLS<sup>Empty vector</sup> and RA-FLS<sup>STAT3C</sup>. Cells expressing GFP displayed green fluorescence. Representative green fluorescent and bright-field microscopy images of RA-FLS<sup>Empty vector</sup> and RA-FLS<sup>STAT3C</sup> are shown in the left panel (Scale bar: 10 μm). Representative immunoblotting results are shown in the right panel. Each membrane was cut based on molecular weights of proteins to be examined before hybridisation with primary antibodies. Original images of all blots are presented in Additional file 5. **(b)** Over-activation of STAT3 attenuated the inhibitory effect of CSR on RA-FLS hyperproliferation. Transduced RA-FLS were incubated with indicated concentrations of CSR for 1 h and then stimulated with IL-6/sIL-6R (100 ng/ml each) for 48 h. Cell viability was assessed using CCK-8 assays. Data are expressed as mean ± SD of 3 independent experiments. Differences of relative cell viabilities between CSR-treated RA-FLS<sup>Empty vector</sup> and CSR-treated RA-FLS<sup>STAT3C</sup> were calculated. \* *P* < 0.05, \*\* *P* < 0.01

apoptosis in, IL-6/sIL-6R-stimulated RA-FLS, substantiating that CSR has anti-arthritic potential.

Apart from STAT3, high expression and over-activation of STAT1, another STAT family member that is related to inflammation, can also be observed in the synovium of RA patients [29]. In the RA-FLS model, STAT1 can also be activated by IL-6/sIL-6R stimulation [30]. Suppressing STAT1 expression and inhibiting STAT1 activation have been regarded as approaches for treating RA [30]. Whether CSR exerts anti-RA effects by inhibiting STAT1 signaling remains to be studied.

Hyper-proliferated FLS interact with bone cells, which is another important event involved in joint damage in RA. IL-6/sIL-6R complex induces RA-FLS hyperproliferation through promoting the autocrine of receptor activator of NF-κB ligand (RANKL) [31]. RANKL facilitates the differentiation of osteoclasts from myeloid precursors, leading to bone erosion [32, 33]. To explore the involvement of RANKL in CSR's anti-RA mechanisms, we will, in the future, investigate whether CSR inhibits RANKL production by suppressing JAK2/STAT3 pathway in IL-6/sIL-6R-stimulated RA-FLS.

## Conclusions

In the present study, we for the first time demonstrated that CSR inhibits hyperproliferation of IL-6/sIL-6R-stimulated RA-FLS, and that inhibition of JAK2/STAT3 signaling is one of the underlying mechanisms. This study provides pharmacological and chemical justifications for the traditional use of CSR-containing herbs in RA treatment, and provides pharmacological groundwork for developing CSR as a novel anti-RA agent. Moreover, this study supports the notion that the JAK2/STAT3 pathway is a target for anti-RA drug discovery.

## Abbreviations

Bcl-2: B-cell lymphoma 2; FLS: Fibroblast-like synoviocytes; GFP: Green fluorescent protein; IL-6: Interleukin-6; JAK2: Janus kinase 2; Mcl-1: Myeloid cell leukemia 1; RA: Rheumatoid arthritis; STAT3: Signal transducer and activator of transcription 3.

## Supplementary Information

The online version contains supplementary material available at <https://doi.org/10.1186/s12906-022-03553-w>.

**Additional file 1.** Effects of CSR on the proliferation of IL-6/sIL-6R-stimulated MIHA and L929 cells. (a) MIHA cell viability. (b) L929 cell viability. In (a) and (b), cells were incubated with indicated concentrations of CSR for 1 hr and then stimulated with IL-6/sIL-6R (100 ng/ml each) for 24 hrs. Cell viability was detected using CCK8 assays. Data are expressed as mean  $\pm$  SD of 3 independent experiments. \*  $P < 0.05$  vs. IL-6/sIL-6R plus CSR solvent-treated group.

**Additional file 2.** Protein levels of STAT3 and phospho-STAT3 (Tyr705) in RA-FLS stimulated with IL-6/sIL-6R (100 ng/ml each) for different durations.  $\beta$ -Actin served as the loading control. Representative immunoblotting results are shown in the left panel. Quantitative results of phospho-STAT3 are shown in the right panel. Data are expressed as mean  $\pm$  SD of 3 independent experiments. \*\*  $P < 0.01$  vs. 0 min group.

**Additional file 3.** Original blot images of immunoblotting results in Fig. 2b. Representative images of cleaved caspase-3, cleaved caspase-9 and GAPDH are shown. Bands are shown on different films because of different exposure time.

**Additional file 4.** Original blot images of immunoblotting results in Fig. 3. Representative images of JAK2, phospho-JAK2 (Tyr1007/1008), STAT3, phospho-STAT3 (Tyr705), STAT3 (cytoplasm), STAT3 (nucleus), Bcl-2, Mcl-1, lamin B1,  $\beta$ -actin and GAPDH are shown. Bands are shown on different films because of different exposure time.

**Additional file 5.** Original blot images of immunoblotting results in Fig. 4. Representative images of Flag, STAT3, phospho-STAT3 (Tyr705) and GAPDH are shown. Bands are shown on different films because of different exposure time.

**Additional file 6.** Original blot images of immunoblotting results in Additional file 2. Representative images of STAT3, phospho-STAT3 (Tyr705) and  $\beta$ -actin are shown. Bands are shown on different films because of different exposure time.

## Acknowledgements

Not applicable.

## Authors' contributions

JYW and YJC participated in experiment design, performed the experiments and data analysis, and drafted the manuscript. XQF, JYC, CLY, JKL, JXB, YW, XQW, ASL and LYW participated in performing the experiments. ZLY designed

the study and finalized the manuscript. All authors read and approved the final manuscript.

## Funding

This work is supported by Shenzhen Science and Technology Innovation Commission (JCYJ20160229210327924, JCYJ20170817173608483 and JCYJ20200109150719846), National Natural Science Foundation of China (81673649, 8187141799 and 81803788), Research Grants Council of Hong Kong (12102918 and 12101519) and Guangdong Provincial Department of Science and Technology (2020A1515010579). These funders had no role in the study design; in the collection, analyses, or interpretation of data, nor in the manuscript preparation.

## Availability of data and materials

All data generated or analyzed during this study are included in this published article, and are available from the corresponding author on reasonable request.

## Declarations

### Ethics approval and consent to participate

Not applicable.

### Consent for publication

Not applicable.

### Competing interests

I declare that the authors have no competing interests as defined by BMC, or other interests that might be perceived to influence the results and/or discussion reported in this paper.

### Author details

<sup>1</sup>Research and Development Centre for Natural Health Products, HKBU Shenzhen Institute of Research and Continuing Education, Shenzhen, China. <sup>2</sup>School of Chinese Medicine, Consun Chinese Medicines Research Centre for Renal Diseases, Hong Kong Baptist University, Hong Kong, China. <sup>3</sup>Centre for Cancer and Inflammation Research, School of Chinese Medicine, Hong Kong Baptist University, Kowloon Tong, Hong Kong, China. <sup>4</sup>JaneClare Transdermal TCM Therapy Laboratory, Hong Kong Baptist University, Hong Kong, China.

Received: 23 April 2021 Accepted: 4 March 2022

Published online: 16 March 2022

## References

- David L. Scott, Frederick Wolfe, Tom W J Huizinga. Rheumatoid arthritis. *Lancet*. 2010;376(9746):1094–108.
- Smolen JS, Aletaha D, McInnes IB. Rheumatoid arthritis. *Lancet*. 2016;388:2023–38.
- Mor A, Abramson SB, Pillinger MH. The fibroblast-like synovial cell in rheumatoid arthritis: A key player in inflammation and joint destruction. *Clin Immunol*. 2005;115:118–28.
- Walker JG, Smith MD. The Jak-STAT pathway in rheumatoid arthritis. *J Rheumatol*. 2005;32:1650–3.
- Gabay C. Interleukin-6 and chronic inflammation. *Arthritis Res Ther*. 2006;8(SUPPL. 2):1–6.
- Burmester GR, Pope JE. Novel treatment strategies in rheumatoid arthritis. *Lancet*. 2017;389(10086):2338–48.
- Smolen JS, Aletaha D, Koeller M, Weisman MH, Emery P. New therapies for treatment of rheumatoid arthritis. *Lancet*. 2007;370:1861–74.
- Tarp S, Furst DE, Boers M, Luta G, Bliddal H, Tarp U, et al. Risk of serious adverse effects of biological and targeted drugs in patients with rheumatoid arthritis: A systematic review meta-analysis. *Rheumatology (Oxford)*. 2017;56:417–25.
- Ruderman EM. Overview of safety of non-biologic and biologic DMARDs. *Rheumatology (Oxford)*. 2012;51(SUPPL. 6):37–43.
- Ravindran V, Rachapalli S, Choy EH. Safety of medium- to long-term glucocorticoid therapy in rheumatoid arthritis: A meta-analysis. *Rheumatology (Oxford)*. 2009;48:807–11.

11. van Walsem A, Pandhi S, Nixon RM, Guyot P, Karabis A, Moore RA. Relative benefit-risk comparing diclofenac to other traditional non-steroidal anti-inflammatory drugs and cyclooxygenase-2 inhibitors in patients with osteoarthritis or rheumatoid arthritis: A network meta-analysis. *Arthritis Res Ther.* 2015;17.
12. Jeyadevi R, Sivasudha T, Rameshkumar A, Kumar LD. Anti-arthritis activity of the Indian leafy vegetable *Cardiospermum halicacabum* in Wistar rats and UPLC-QTOF-MS/MS identification of the putative active phenolic components. *Inflamm Res.* 2013;62:115–26.
13. Kim C, Kim MC, Kim SM, Nam D, Choi S H, Kim SH, et al. Chrysanthemum indicum L. extract induces apoptosis through suppression of constitutive STAT3 activation in human prostate cancer DU145 cells. *Phytother Res.* 2013;27:30–8.
14. Ananth DA, Rameshkumar A, Jeyadevi R, Aseervatham GSB, Sripriya J, Bose PC, et al. Amelioratory effect of flavonoids rich *Pergularia daemia* extract against CFA induced arthritic rats. *Biomed Pharmacother.* 2016;80:244–52.
15. Chen XY, Li J, Cheng WM, Jiang H, Zhang L, Hu R. Effect of total flavonoids from chrysanthemum indicum on ultrastructure and secretory function of synoviocytes in adjuvant Arthritis Rats. *Lat Am J Pharm.* 2011;30:2031–6.
16. Wu JY, Chen YJ, Bai L, Liu YX, Fu XQ, Zhu PL, et al. Chrysoeriol ameliorates TPA-induced acute skin inflammation in mice and inhibits NF- $\kappa$ B and STAT3 pathways. *Phytomedicine.* 2020;68.
17. Tse AKW, Chen YJ, Fu XQ, Su T, Li T, Guo H, et al. Sensitization of melanoma cells to alkylating agent-induced DNA damage and cell death via orchestrating oxidative stress and IKK $\beta$  inhibition. *Redox Biol.* 2017;11:562–76.
18. Chen YJ, Liu YX, Wu JY, Li CY, Tang MM, Bai L, et al. A two-herb formula inhibits hyperproliferation of rheumatoid arthritis fibroblast-like synoviocytes. *Sci Rep.* 2021;11:1–9.
19. Nowell MA, Richards PJ, Horiuchi S, Yamamoto N, Rose-John S, Topley N, et al. Soluble IL-6 Receptor Governs IL-6 Activity in Experimental Arthritis: Blockade of Arthritis Severity by Soluble Glycoprotein 130. *J Immunol.* 2003;171:3202–9.
20. Nishimoto N, Terao K, Mima T, Nakahara H. Mechanisms and pathologic significances in increase in serum interleukin-6 (IL-6) and soluble IL-6 receptor after administration of an anti-IL-6 receptor antibody. *Blood.* 2008;112:3959–65.
21. Hashizume M, Mihara M. The roles of interleukin-6 in the pathogenesis of rheumatoid arthritis. *Arthritis.* 2011;2011:765624.
22. Johnson DE, O'Keefe RA, Grandis JR. Targeting the IL-6/JAK/STAT3 signaling axis in cancer. *Nat Rev Clin Oncol.* 2018;15:234–48.
23. Hodge DR, Hurt EM, Farrar WL. The role of IL-6 and STAT3 in inflammation and cancer. *Eur J Cancer.* 2005;41:2502–12.
24. Carpenter RL, Lo HW. STAT3 target genes relevant to human cancers. *Cancers.* 2014;6:897–925.
25. Bartok B, Firestein GS. Fibroblast-like synoviocytes: Key effector cells in rheumatoid arthritis. *Immunol Rev.* 2010;233:233–55.
26. Noss EH, Brenner MB. The role and therapeutic implications of fibroblast-like synoviocytes in inflammation and cartilage erosion in rheumatoid arthritis. *Immunol Rev.* 2008;223:252–70.
27. Krause A, Scaletta N, Ji J-D, Ivashkiv LB. Rheumatoid Arthritis Synoviocyte Survival Is Dependent on Stat3. *J Immunol.* 2002;169:6610–6.
28. Kyung Chang S, Gu Z, Brenner MB. Fibroblast-like synoviocytes in inflammatory arthritis pathology: The emerging role of cadherin-11. *Immunol Rev.* 2010;233:256–66.
29. Kasperkovitz P v, Verbeet NL, Smeets TJ, van Rietschoten JGI, Kraan MC, et al. Activation of the STAT1 pathway in rheumatoid arthritis. *Ann Rheum Dis.* 2004;63:233–9.
30. Ikari Y, Isozaki T, Tsubokura Y, Kasama T. Peficitinib Inhibits the Chemotactic Activity of Monocytes via Proinflammatory Cytokine Production in Rheumatoid Arthritis Fibroblast-Like Synoviocytes. *Cells.* 2019;8:561.
31. Hashizume M, Hayakawa N, Mihara M. IL-6 trans-signalling directly induces RANKL on fibroblast-like synovial cells and is involved in RANKL induction by TNF- $\alpha$  and IL-17. *Rheumatology.* 2008;47:1635–40.
32. Gravallese EM, Manning C, Tsay A, Naito A, Pan C, Amento E, et al. Synovial tissue in rheumatoid arthritis is a source of osteoclast differentiation factor. *Arthritis Rheum.* 2000;43:250–8.
33. Bottini N, Firestein GS. Duality of fibroblast-like synoviocytes in RA: Passive responders and imprinted aggressors. *Nat Rev Rheumatol.* 2013;9:24–33.

## Publisher's Note

Springer Nature remains neutral with regard to jurisdictional claims in published maps and institutional affiliations.

**Ready to submit your research? Choose BMC and benefit from:**

- fast, convenient online submission
- thorough peer review by experienced researchers in your field
- rapid publication on acceptance
- support for research data, including large and complex data types
- gold Open Access which fosters wider collaboration and increased citations
- maximum visibility for your research: over 100M website views per year

**At BMC, research is always in progress.**

Learn more [biomedcentral.com/submissions](https://biomedcentral.com/submissions)

